CrossMark

# Study of Surface-Enhanced Raman Scattering of Plasmonic Coupled Biomolecule: Role of Multi-Layered Nanosphere

Gyanendra Krishna Pandey[1,2] · Nilesh Kumar Pathak[1] · R. Uma[1] · R. P. Sharma[1]

**Abstract** In this communication, we study the surface enhanced Raman scattering (SERS) by a molecule which is adsorbed on a trilayer (Ag@SiO$_2$@Ag) spherical shaped metallic nanostructure. We have studied the plasmonic signature of the trilayer nanostructure under quasi-static approximation. The plasmonic response of trilayer nanostructures is analysed in terms of surface plasmon resonances and extinction efficiency which is a function of size, shape of core-shell material and thickness polarisability. The polarisability of trilayer nanostructure has been derived using T-matrix method and coupled it with the Gersten-Nitzan model to study the Raman enhancement factor. The Raman enhancement factor ($R$) has been studied under the influence of several parameters such as core-shell material, thickness, molecule distance and the surrounding media. The model developed here suggests strong relative amplification of the Raman gain of biomolecule adsorbed on the surface of the nanogeometry. The trilayer metal nanostructure exhibits three plasmon resonance peaks in UV to visible range (Raman spectroscopy range) which helps in detection of biological molecules into three different regimes. We have also compared the Raman enhancement factor for trilayer, bilayer and single metal nanosphere and it was observed that the magnitude of Raman gain factor, number of resonant peaks and its spectral bandwidth are different for different geometries.

**Keywords** SERS · Trilayer nanoparticle · SPR · Raman enhancement factor · Biomolecule · Plasmonics

✉ Gyanendra Krishna Pandey
gyanendraiitd@gmail.com

[1] Plasma Simulation Laboratory, Centre for Energy Studies, Indian Institute of Technology, Delhi 110016, India

[2] Shivaji College, University of Delhi, Delhi 110027, India

## Introduction

Surface-enhanced Raman scattering (SERS) is a very efficient and highly sensitive technique for the identification of low concentration molecular species which is an extension of tradition Raman spectroscopy [1, 2]. This SERS technique characterised by enhancement in the Raman signal intensity by the order of the magnitude of a molecule adsorbed on the roughened surface with respect to the molecule adsorbed on the smooth surface [3]. When the electromagnetic wave interacts with the smooth metal surface, the energy associated to the system, flows along the tangential direction and hence the surface-enhanced Raman scattering (SERS) effect is not so significant. When the surface of chosen system is roughened, the electromagnetics of irradiated light becomes very interesting. In this situation, the surface plasmons are excited due to the interaction of conduction electrons of nanoparticle with incident light field and the resulting enhancement in the normal component of electric field of the electromagnetic radiation close to the surface has been observed. As the associated intensity of signal depends on the square of the amplitude of incident light field and hence the intensity is enhanced as compared to what it was without surface [4, 5]. Due to this enhancement in intensity, corresponding Raman scattered (inelastic scattering) field may also be enhanced, but the magnitude of scattered Raman signal is different than that of the incident light field. The net increment associated with the incident and the scattered field is considered to be the electromagnetic contribution to surface-enhanced Raman scattering. An important feature of SERS mechanism is that, it depends on the frequency of Raman signal, size and shape of the metal nanoparticles and surrounding medium. The noble metal nanoparticle's surface plasmon resonances (SPRs) depend on the shape, size and medium which are the main causes of electromagnetic field enhancement near the metallic surface.

The enhanced electromagnetic fields can be utilised for various purposes such as SERS, florescence and bio-sensing [6]. Also, the spectral width, position and intensity of the SPR can be easily tuned for SERS application by changing the parameters like dimension of particle, coating thickness and choice of materials and embedding medium. The various noble metal nanogeometries like coated and noncoated spheres, spheroids and dimers are used to study the electromagnetics of SERS. Out of these geometries, core-shell (for different geometries) has several exciting features like resonance scattering, peak shifting, absorption and intense near-field enhancement, sensitivity and the enhanced frequency domain. Due to these significant features, the plasmonic nanogeometries have wide applications at nanoscale which range from biological and chemical sensing to light trapping in thin film [7–9].

As compared to mono and bilayer metal nanoparticles, trilayer (metal/dielectric/metal) nanosphere is more significant because it exhibits an additional degree of freedom in plasmonic peaks. This extra degree of freedom in SPR occurs due to trilayer nanogeometry which can be utilised more affectively to enhance the Raman gain factor. There are three different Raman peaks that are observed corresponding to trilayer nanogeometry in three different frequency regimes.

In this paper, we have studied the SERS mechanism via trilayer metal nanostructures. The trilayer geometry is a combination of metal@dielectric@metal (Ag@SiO$_2$@Ag). The wavelength-dependent dielectric constant of metal has been taken from the literature [10]. In this layered structures, the choice of coating materials is not arbitrary, two materials can be used as core-shell only if its lattice parameters are nearly equal. It is one of the very important conditions for the coating on the nanogeometry [11, 12]. The schematic diagram of trilayer metal nanostructure is shown in Fig. 1.

## Theory

The electromagnetic mechanism of SERS of the dipole equivalent of biomolecule which is situated at a distance $d$ from the surface of trilayer metal nanostructure has been studied. The electromagnetic behaviour of trilayer metal nanostructure associated with the polarisability which is derived under dipolar model. When a light of electric field intensity E$_0$ interact with the chosen nanogeometry, it scattered light with amplified field intensity. This amplified field intensity interacts inelastically with the biomolecule which is considered to be an equivalent dipole which generates a new signal known as Raman signal. As the interaction is inelastic, the new signal will have a different frequency with respect to the incident one. This Raman signal again interacts with the nanogeometry and reradiate a signal with amplified intensity which is known as SERS signal and the phenomena is called enhanced inelastic Raman scattering. The whole SERS mechanism has been
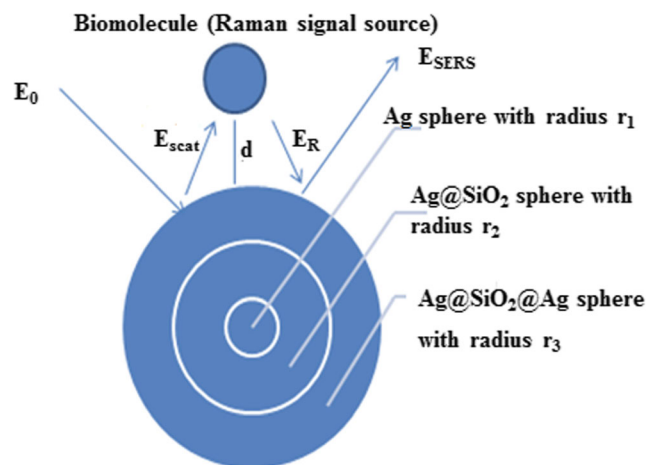


**Fig. 1** Schematic diagram of SERS mechanism of biomolecule which is placed at certain distance $d$ from surface of trilayer plasmonic nanogeometry (Ag@SiO$_2$@Ag)

studied by using Gersten-Nitzan model which is used to find the Raman scattering cross section of composite (metal nanogeometry-biomolecule) system is expressed as [3, 13–17]

$$\sigma_{\text{SERS}} = \left(\frac{8\Pi}{3}\right)\left(\frac{\omega}{c}\right)^4 (\Delta C)^2 \left(\frac{\partial \alpha}{\partial C}\right)^2 \left|\frac{1}{1-\alpha G}\left[1 + \frac{2\alpha_m}{(r_m+d)^3}\right]\right|^4 \quad (1)$$

$$G = \sum_l \frac{(l+1)^2}{(r_m+d)^{2(l+1)}} \alpha_m \quad (2)$$

where $\Delta\alpha$ is the change in polarisability of molecule which occurs due to is change in nuclear coordinate " $\Delta C$ ". $G$ is image field factor which depends on the morphology. The molecular polarisability is assumed to be constant, $r_m$ is the radius of multi-layered nanosphere and $l$ is the running index with $l=1$ for dipole case. Hence, the Raman enhancement factor of biomolecule which is separated by distance $d$ from the plasmonic nanogeometry can be expressed as

$$R = \left|\frac{1}{1-\alpha G}\left[1 + \frac{2\alpha_m}{(r_m+d)^3}\right]\right|^4 \quad (3)$$

where $\alpha_m$ the dipolar polarisability of the metal nanostructure, $\omega$ is the incident light frequency, $c$ is the speed of light in free space and $\alpha$ is the polarisability of chosen biomolecule which is constant and of the order of angstrom$^3$. Generally, the polarisability of small organic molecule is in the range of 1–10 angstrum$^3$ [3]. This polarisability plays a very significant role to understand the resonance physics and its expression is different corresponding to the different nanogeometries. In the polarisability $\alpha_m$, the subscript

$m = 1$ for isolated metal nanosphere, $m = 2$ stands for bilayer and $m = 3$ for trilayer. The polarisability of noncoated and coated metal nanosphere is obtained by using dipole model, while the polarisability of trilayer nanosphere is derived by using T-matrix method.

For the analysis of single, bi- and trilayer metal nanosphere, we assume that the nanoparticle is irradiated by oscillating electromagnetic field which is spatially uniform. Here, Laplace equation is used to find out the potential, field and polarisability expression [6]. A single, isolated metal nanosphere which is embedded in a homogeneous medium has constant electric field. The polarisability of sphere is expressed as

$$\alpha_s = 4\pi r_1^3 \left| \frac{\varepsilon_1 - \varepsilon_m}{\varepsilon_1 + 2\varepsilon_m} \right| \tag{4}$$

where $\varepsilon_m$ is the dielectric constant of surrounding media, $\varepsilon_1$ is the dielectric constant of silver MNPs, '$r_1$' is the radius of isolated nanosphere.

Consider the coated nanoparticle (Ag@SiO$_2$) embedded in ambient matrix of dielectric constant $\varepsilon_m$. The polarisability of coated nanoparticle is expressed as [14]

$$\alpha_{bi} = 4\pi r_2^3 \frac{(\varepsilon_2 - \varepsilon_m)(\varepsilon_1 + 2\varepsilon_2) + f(\varepsilon_1 - \varepsilon_2)(\varepsilon_m + 2\varepsilon_2)}{(\varepsilon_2 + 2\varepsilon_m)(\varepsilon_1 + 2\varepsilon_2) + f(2\varepsilon_2 - 2\varepsilon_m)(\varepsilon_1 - \varepsilon_2)} \tag{5}$$

where $r_2$ is the outer sphere radius, $\varepsilon_m$ is the dielectric constant of the medium, $\varepsilon_1$ is the dielectric constant of inner sphere (silver metal), $\varepsilon_2$ is the dielectric constant of shell (silica).

Under the same situation as discussed above, consider three layer core-shell nanosphere embedded in homogeneous medium is irradiated by field. After the interaction of light with trilayer nanosphere, the $l$th polarisability expression of this nanosphere has been found using T-matrix method which is expressed as [14, 15].

$$\alpha_{tri} = \frac{\mathrm{Num}\alpha_1}{\mathrm{Den}\alpha_1} \tag{6}$$

where, $\alpha_{tri}$ is the ratio of numerator $\alpha_l$ to denominator $\alpha_l$ represents, $\alpha_l$ is the polarisability of $l$th layer nanosphere and for dipole approximation, we have only considered $l = 1$ which can be expressed as

$$\begin{aligned}\mathrm{Num}\alpha_1 = r_3^3 \Big[ \varepsilon_1 \Big( \varepsilon_2 \big[ 2r_1^3 + r_2^3 \big] \{ r_2^3[(\varepsilon_3 + \varepsilon_m) + \varepsilon_3] + (\varepsilon_3 - \varepsilon_m)r_3^3 \} \\ + \varepsilon_3(r_2^3 - r_1^3) \{ -r_2^3[(\varepsilon_3 + \varepsilon_m) + \varepsilon_3] + 2(\varepsilon_3 - \varepsilon_m)r_3^3 \} \Big) \\ + \varepsilon_2 \Big( \varepsilon_3 [r_1^3 + 2r_2^3] \{ -r_2^3[(\varepsilon_3 + \varepsilon_m) + \varepsilon_3] + 2(\varepsilon_3 - \varepsilon_m)r_3^3 \} \\ - 2\varepsilon_2(r_1^3 - r_2^3) \{ r_2^3[(\varepsilon_3 + \varepsilon_m) + \varepsilon_3] + (\varepsilon_3 - \varepsilon_m)r_3^3 \} \Big) \Big]\end{aligned}$$

and

$$\begin{aligned}\mathrm{Den}\alpha_1 = \varepsilon_1 \Big( \varepsilon_2 \big[ 2r_1^3 + r_2^3 \big] \{ 2 \big[ (\varepsilon_3 - \varepsilon_m)r_2^3 + r_3^3[(\varepsilon_3 + \varepsilon_m) + \varepsilon_m] \big] \} \\ + 2\varepsilon_3(r_2^3 - r_1^3) \{ (\varepsilon_m - \varepsilon_3)r_2^3 + r_3^3 \big[ (\varepsilon_3 + \varepsilon_m) + \varepsilon_m \big] \} \Big) \\ - 2\varepsilon_2 \Big( \varepsilon_2(r_1^3 - r_2^3) \{ 2 \big[ (\varepsilon_3 - \varepsilon_m)r_2^3 + r_3^3(\varepsilon_3 + \varepsilon_m) + \varepsilon_m \big] \} \\ + \varepsilon_3 [r_1^3 + 2r_2^3] \{ (\varepsilon_3 - \varepsilon_m)r_2^3 + r_3^3[(\varepsilon_3 + \varepsilon_m) + \varepsilon_m] \} \Big)\end{aligned}$$

where $r_1$, $r_2$ and $r_3$ are the radii of the inner, middle and outer layer sphere having dielectric constants $\varepsilon_1$, $\varepsilon_2$ and $\varepsilon_3$, respectively.

First, we find the polarisability expression for the chosen nanogeometries after then we able to find the optical signatures like absorption, extinction and scattering of MNPs under the condition of quasi-static approximation expressed as [14]

$$C_{\mathrm{scat.}} = \frac{k^4}{6\pi} |\alpha_m|^2; k = \frac{2\pi}{\lambda} \tag{7}$$

$$C_{\mathrm{absa}} = k \mathrm{Im}(\alpha_m) \tag{8}$$

$$Q_{\mathrm{ext}} = \frac{(C_{\mathrm{scat}} + C_{\mathrm{absa}})}{\pi r_i^2} \tag{9}$$

In these equations (7, 8), polarisability $\alpha_m$ depends on dielectric constant of dielectric material (silica) and metal (silver). To involve the nano effect, size-dependent dielectric constant metal has been considered which is derived from Drude Lorentz model, that can be expressed as [18, 19]

$$\varepsilon(\omega) = \varepsilon_{\mathrm{bulk}}(\omega) + \frac{\omega_p^2}{\omega^2 + j\gamma_{\mathrm{bulk}}\omega} - \frac{\omega_p^2}{\omega^2 - j\gamma\omega} \tag{10}$$

$$\gamma = \gamma_{\mathrm{bulk}} + A\frac{v_f}{r_m} \tag{11}$$

$$\tau = 1 \big/ \gamma, \tau_{\mathrm{bulk}} = 1 \big/ \gamma_{\mathrm{bulk}} \tag{12}$$

where $\gamma$ is the effective relaxation time, $\gamma_{\mathrm{bulk}}$ is the free electron scattering time of bulk metal, $v_f$ ($1.39 \times 10^6$ m/s) is the electron Fermi velocity in silver metal, and $A$ is a geometry-dependent parameter which lies between 1 to 3 [7]. The variable $r_m$ represents the radius of the chosen metal nanosphere which clearly makes the difference bulk level property and nanolevel property. When the radius of metal nanosphere increases then the second part of Eq. (11) plays no significant role, the damping at nanolevel and bulk level is nearly equal. Under this condition, there is no distinction between the optical constant between at nanolevel and bulk level.

## Results and Discussion

The optical properties of trilayer metal nanostructure has been analysed in terms of polarisability expression which is derived by using t-matrix method. After the complete analysis of polarisability of trilayer nanostructure, we couple this expression into GN model to find out the Raman enhancement factor. The multi-layered metal nanostructure would exhibit entirely different optical properties to the bilayer and simple metal sphere and these properties are analysed in terms of surface plasmon resonances. The coupling of light with the trilayer metal nanostructure under the influence of biomolecule (which is placed at distance $d$ from the surface of metal nanogeometry) plays a very significant role to enhance the Raman signal. The enhancement in the Raman signal studied in terms of Raman enhancement factor as indicated by (Eq. 3). Figure 2 represents the Raman enhancement spectra of trilayer (Ag@SiO$_2$@Ag) metal nanostructures against the incident light frequency normalised by plasmon frequency. In Fig. 2, the two outer radii $r_2$ and $r_3$ are fixed and inner radius $r_1$ is variable. The trilayer metal nanostructure embedded in two surrounding environments air and water with refractive index $N = 1$ and $N = 1.32$ respectively as shown in Fig. 2 a, b. As increasing core radius $r_1$ with fixed $r_2 = 20$ nm, $r_3 = 25$ and $d = 1$ nm, corresponding Raman enhancement factor increases in different regimes of frequency. The consistent increment in the Raman enhancement factor with the core radii is observed due to the reduction in thickness of shell. The interaction of light with trilayer nanosphere exhibits three plasmon resonances in three different frequency ranges which are utilised to amplify the Raman signal at three different points of whole

frequency domain. When the resonance frequency of the nano geometry matches with the electronic transition frequency which occurs in different electronic and corresponding vibrational level of the molecule, the coincided range of the frequency get amplified.

Figure 3 represents the frequency-dependent Raman enhancement spectra of trilayer metal nanosphere embedded in two different environments. Here, inner and outer layer radii ($r_1$ and $r_3$) are fixed while the middle layer (silica) radius $r_2$ is variable. In Fig. 3, when the radius of the silica changes, the effective dielectric constant of the system changes which allows shifting in the resonance peaks and hence there will be corresponding shift in the enhancement factor. For particular case of multilayer nanosphere where $r_1 = 15$ nm, $r_2 = 18$ nm and $r_3 = 25$ nm with $N = 1$, the enhancement peak is obtained at the normalised frequency 0.31 as shown in Fig. 3a, and when the surrounding medium changes from $N = 1$ to $N = 1.32$ (keeping all parameters constant), the enhancement peak was observed at the normalised frequency to 0.28. It was observed that the resonance peaks shift towards the red region as we increase the surrounding dielectric constant and the corresponding enhancement factor also changes. Since the SERS enhancement factor is a function of polarisability that depends on the various physical parameters like shape, size and surrounding materials, any change in the surrounding materials will cause a change in SERS enhancement factor. The physics of peak shifting with surrounding media can be understood by using relation $\omega = \omega_p/\sqrt{1-\varepsilon_p} = \omega_p/\sqrt{1+2\varepsilon_m}$ where $\omega_p$ is the plasmon frequency of the conduction electrons of nanosphere, $\varepsilon_p$ is the dielectric constant of the nanoparticle
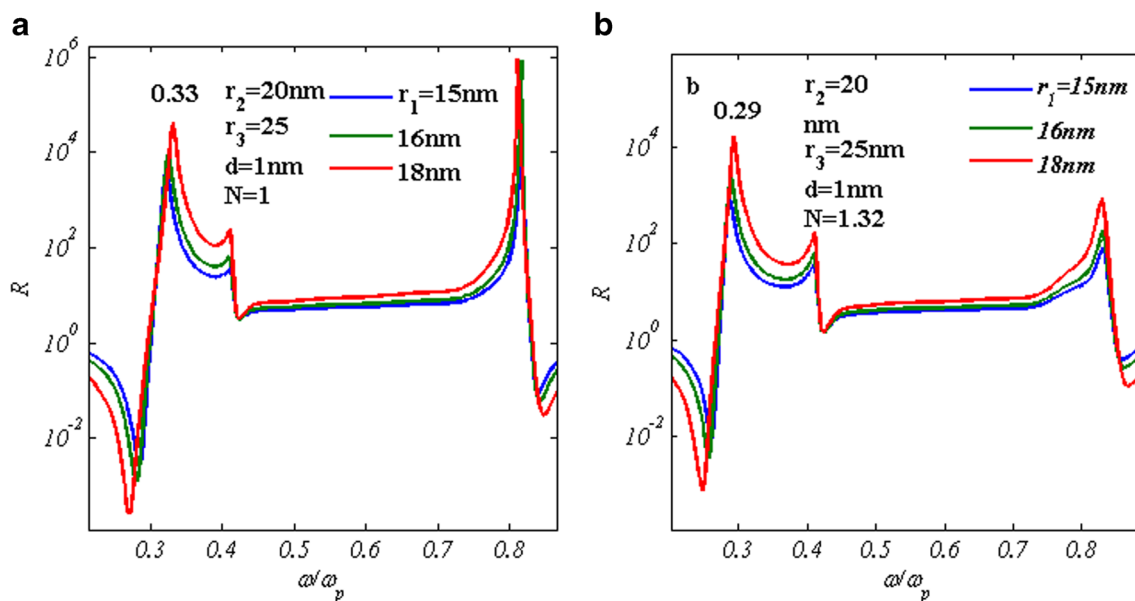


**Fig. 2** Raman enhancement factor ($R$) of plasmonic coupled biomolecule which is a function of normalised plasmon frequency for trilayer MNP (Ag@SiO$_2$@Ag) with radii 15/20/25 embedded in two different environments having refractive index $N = 1$ and $N = 1.32$. The inner radii are variable with constant value of $d$, where $d$ is the distance between molecule and the top of nanogeometry
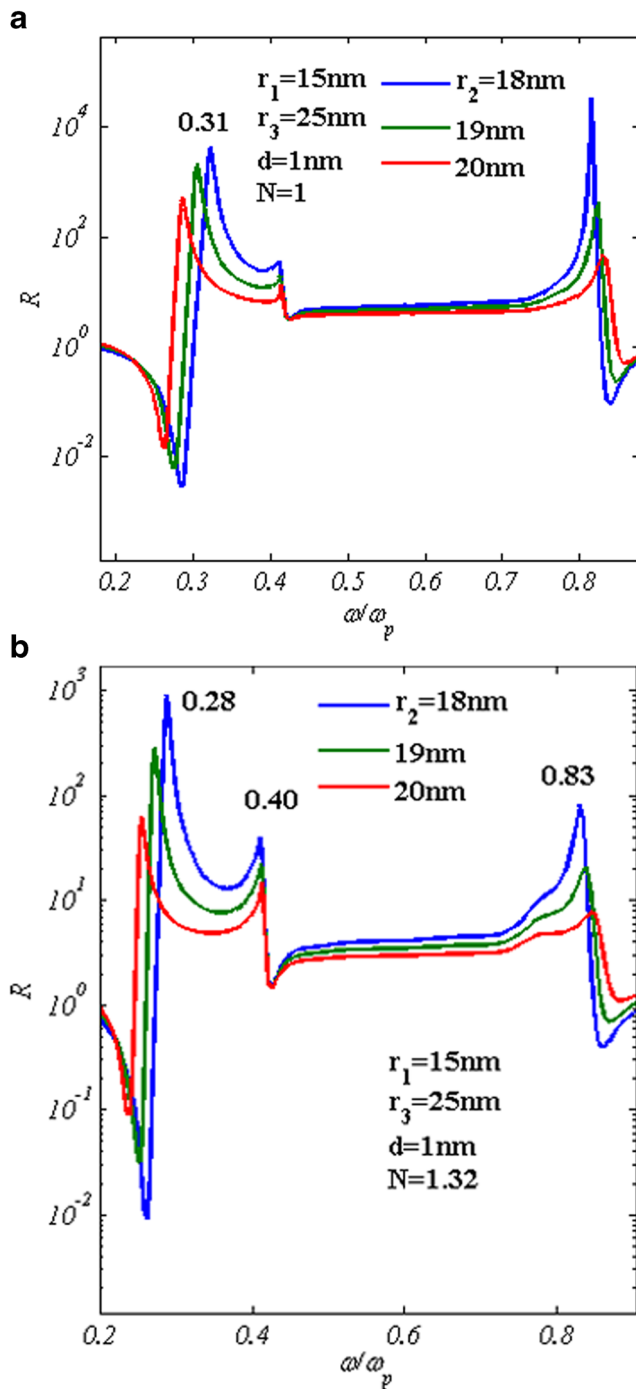
**a**



**b**



**Fig. 3** Raman enhancement factor ($R$) of plasmonic coupled biomolecule which is a function of normalised plasmon frequency for trilayer MNP (Ag@SiO$_2$@Ag) with radii 15/20/25 embedded in two different environment having refractive index $N = 1$ and $N = 1.32$. The inner radius $r_2$ is variable with fixed value of molecule distance from the surface of nanosphere ($d = 1$ nm)

and $\varepsilon_m$ is the dielectric constant of surrounding medium. From this expression, it is clear that when dielectric constant of the surrounding medium $\varepsilon_m$ increases, the frequency of oscillation $\omega$ decreases i.e., red shifting of the LSP resonance peak and hence red shifting of Raman enhancement peak. In this figure,

peaks are observed due to the antisymmetric and symmetric coupling of higher and lower frequency modes, respectively [18, 19]. The antisymmetric mode generation at higher frequency is the effect of the antibonding resonance in which the surface charge oscillations, at the interface of the two different media coupled antisymmetrically, while the symmetric mode is because of the symmetric coupling.

The Raman enhancement factor of biomolecule under trilayer nano plasmonic effects plotted against normalised frequency is shown in Fig. 4. Here, we analyse how the molecule distance from the surface of trilayer metal nanosphere would influence the Raman gain factor. In Fig. 4, we change the distance $d$ from the surface of the multi-layered nanogeometry (silver-silica-silver) and studied the Raman enhancement factor $R$ with respect to the normalised frequency in the range from UV to near IR reason. In the result, we find three picks that have already observed in the previous case. The appearance of these three picks is due to the three interfaces where surface plasmons are excited separately at each interface [20, 21]. The separate excitation of SPRs in different frequency domain resonantly enhanced the local field which is responsible to increase the intensity of Raman signal. In the figure, it can be easily seen that the Raman gain factor is directly proportional to the distance $d$. The enhancement factor is higher for the closer distance between the molecule and the plasmonic geometry and it is lower when the distance $d$ is increase from the nanogeometry. The molecules which are far away from the surface of metal nanosphere are not going to experience plasmonic local field that is why the reduction in the Raman gain factor was observed. Hence, for better amplification in Raman gain via SERS technique, the distance between biomolecule and plasmonic nanogeometries is not very far away from each other.

Figure 5 shows the extinction efficiency of the trilayer metal nanosphere with respect to normalised wavelength ($\lambda/\lambda_p$) for two different values of $r_1 = 15$ and 17 nm having fixed values of $r_2 = 20$ nm and $r_3 = 25$ nm. The chosen nanostructures were embedded in two different dielectric environment having constant refractive index $N = 1$ and 1.32. The extinction spectrum has been plotted to get the idea of SPR peak position and its spectral width. I would like to emphasize the actual meaning of extinction which represents the attenuation of electromagnetic waves as it propagates inside the medium. In simpler fashion, when light interacts with the nanostructures, some parts of it gets absorbed and also scattered and some fraction of light gets detected at the detector. Hence, the sum of absorbed and scattered portion of light by the metal nanogeometry is known as extinction. For the present case, trilayer metal nanostructure three peaks were observed in three different part of electromagnetic spectrum which helps us to study Raman enhancement factor. As we know, the surrounding media would influence the optical properties like SPRs peak position, width and magnitude which can be clearly seen in Fig. 5a, b.
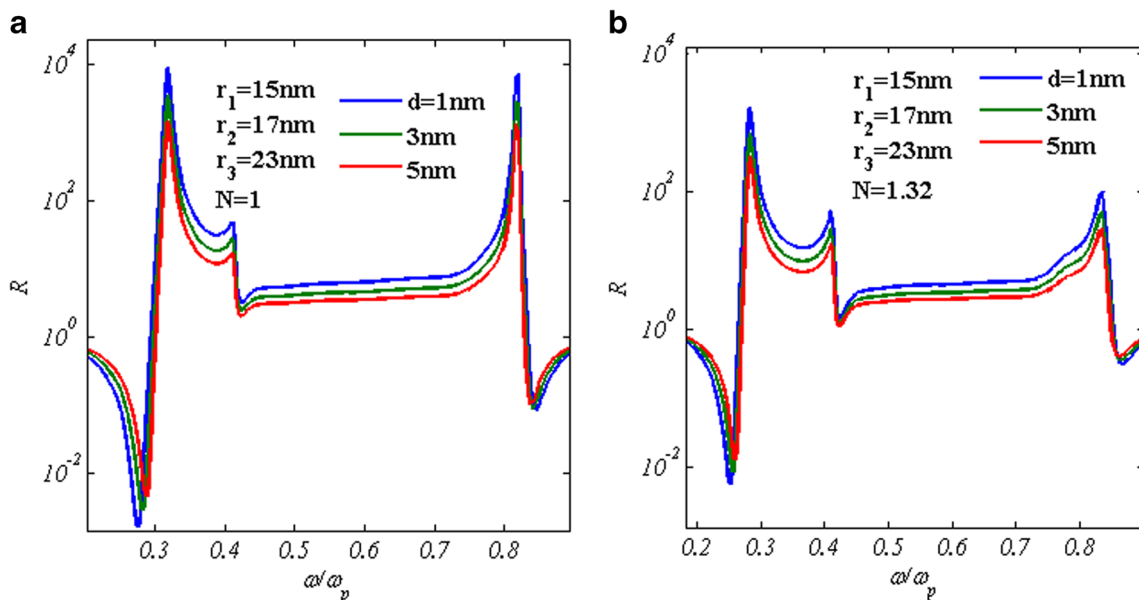
**Fig. 4** Raman enhancement factor ($R$) of plasmonic coupled biomolecule which is a function of normalised plasmon frequency for trilayer MNP (Ag@SiO$_2$@Ag) with radii 15/17/23 embedded in two different environments having refractive index $N = 1$ and $N = 1.32$. The inner, middle and outer radii are fixed and distance $d$ between biomolecule and metallic nanogeometry is variable

Now, we will try to make the comparison between Raman enhancement factor corresponding to three different metal nanostructures which are embedded in air as shown in Fig. 6. Figure 6 represents the Raman intensity amplification factor ($R$) w.r.t normalised frequency for three different situations such as monolayer, bilayer and trilayer metal nanosphere. These metallic nanogeometry embedded in surrounding media with index of refraction $N = 1$. For all the cases, we select core radius 10 nm with $d = 1$ nm. It was observed that when there is no coating on the metal nanoparticle, enhancement factor is smaller in comparison to the system when it is coated as shown in Fig. 6b and the tunability in comparison to the coated nanogeometry is almost negligible. When the system is trilayered, the enhancement factor is different with some additional feature which appeared in the form of third resonance peak as shown in the Fig. 6c. The advantage of trilayer nanosphere is that there are three resonant peaks observed which will be utilised to amplify the Raman signal three times at three different positions of frequency domain.
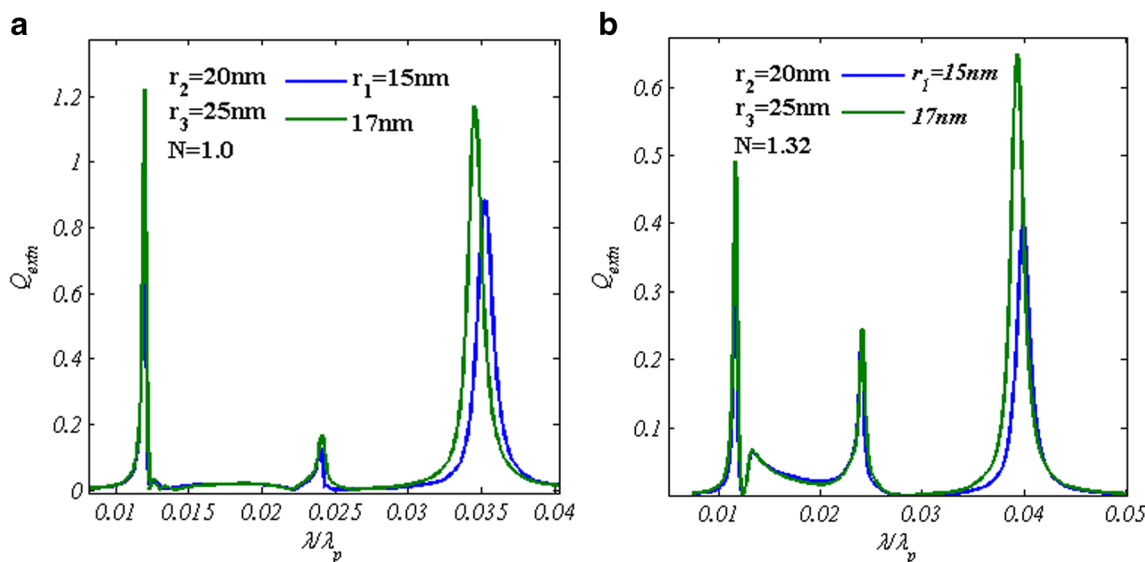


**Fig. 5** The extinction efficiency of the trilayer metal nanosphere with respect to normalised wavelength ($\lambda/\lambda_p$) for two different values of $r_1 = 15$ and 17 nm having fixed values of $r_2 = 20$ nm and $r_3 = 25$ nm
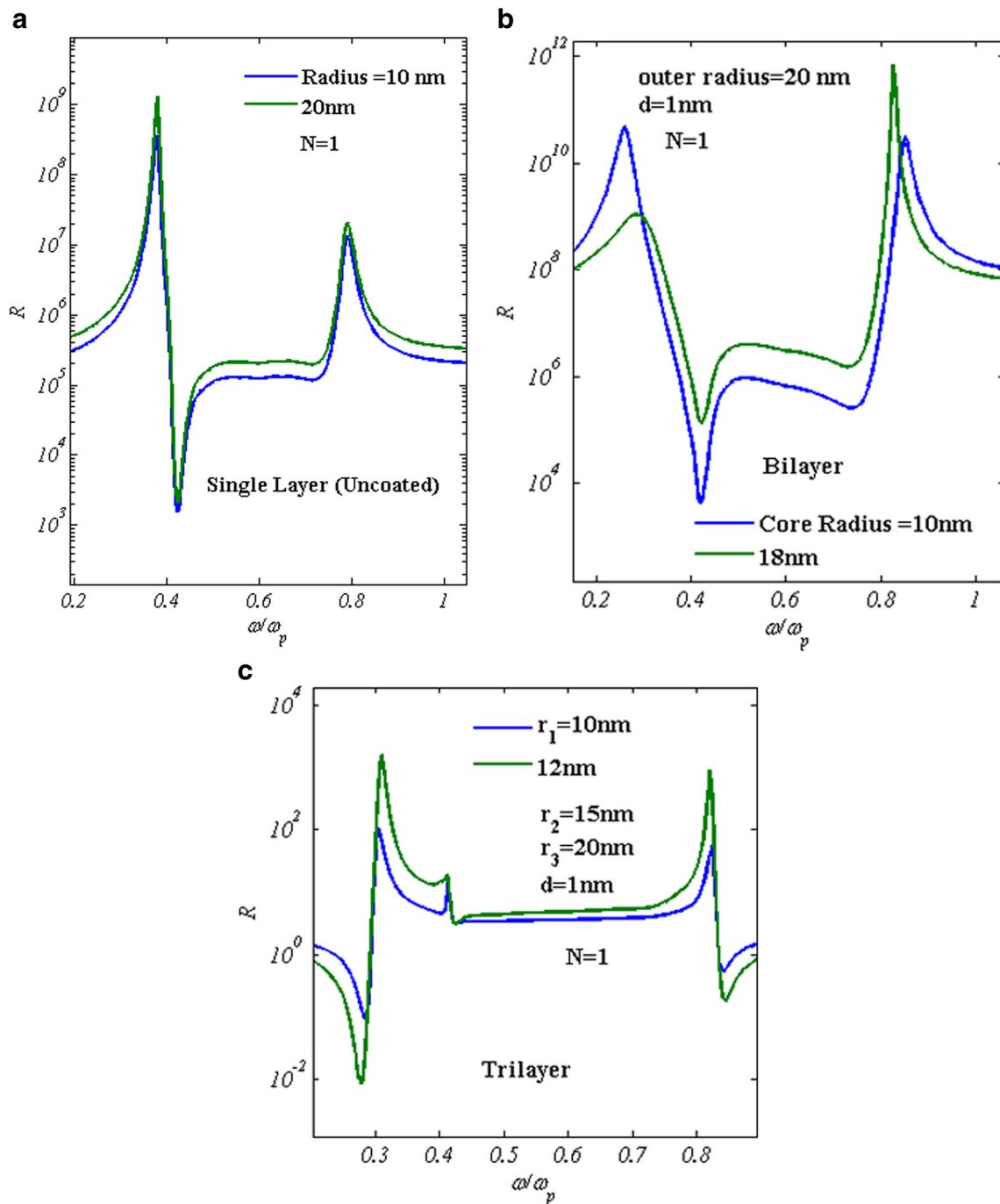
**Fig. 6** The Raman enhancement spectra of sphere, core-shell bilayer (Ag@Sio2) and core-shell trilayer metal nanosphere (Ag@Sio2@Ag) against normalised plasmon frequency. In all cases, nanosphere embedded in air of $N = 1$ and $d = 1$ nm

It was also observed that, in all three cases, damping in the resonance frequency is governed by the expression $\gamma = \gamma_{bulk} + Av_f/R_{eff}$. The term $R_{eff}$ is $r_1$ for noncoated nanosphere and $R_{eff}$ is $r_2 - r_1$ for coated system [22–29]. If $R_{eff}$ is higher, higher is the collision time of electron and lower will be thee damping and vice versa. In case of noncoated nanospherical geometry, the resonance peak abruptly changes due to the damping effects. It takes minimum frequency difference to become zero

which means taking longer time difference and hence low damping factor. Now, let us consider second case. In this, there are two systems, one bilayer and other is trilayer. In the case of bilayer in Fig. 6b, the resonance peak takes longer frequency difference in comparison to the trilayer geometry Fig. 6c, because in bilayer situation electrons collision frequency is higher because of small expansion of the boundary of the coating and hence high damping value. At the same time,

because of higher extension of material boundary, smaller collision frequency and hence high relaxation time lead to smaller damping coefficient and hence enhancement peak takes smaller time to come to its normal situation. The reason behind this effect may be explained by equation $\gamma = \gamma_{bulk} + Av_f/r_m$, where, the second part of the denominator represents the shell thickness of the nanogeometry. In the case of Fig. 6a, there is no coating and hence shell thickness is almost zero; this leads to very high collision frequency and hence the effective damping factor is very high. This results in very fast energy dissipation of SPR resonance peak and fast decay of the resonance peak.

## Conclusions

In this paper, we have followed electromagnetic approach for the analysis of SERS theory of biomolecule used as an adsorbate on the surface of trilayer metal nanosphere. We derived the polarisability expression for the trilayer nanospherical geometry ($Ag@SiO_2@Ag$) to study the Raman enhancement factor. We here observe that, for the trilayer coated nanospherical geometry, there are three resonant peaks in the normalised frequency domain for the different optimised parameters, like layer thickness, radius of nanosphere and surrounding medium. We also have compared the results by changing the surrounding media, in which, the whole system is kept. For the case where the molecule is in water-like concentration, the enhancement in the Raman gain was observed, as compared to the case when it is in free space. It was also compared with the results of the previous, where the observations for uncoated and single-coated metal nanoparticle case were discussed for the biomolecule detection. We also have discussed the extinction spectrum against the normalised wavelength for the nanoplasmonic system to get the idea of resonance wavelength. In the last part of this communication, there is a comparison of enhancement factor ($R$) for different conditions have been done. As we know, disease detection needs identification of biomolecule. The effective diagnosis even today is a challenge in medical field. There are so many physical and chemical methods available in diagnosis field, which have their own advantages with some limitations. Hence, the present modelling approach opens new platform that will help the scientific community to study the enhancement and tunability of Raman gain signal by changing the various parameters.

## References

1. Won WH, Cheong H (2016) Exploring surface enhanced Raman scattering background using a sandwiched graphene monolayer with gap plasmon junction. J Phys D Appl Phys 49:105302–105305
2. Kelly KL, Coronado E, Zhao L, Schatz GC (2003) The optical properties of metal nanoparticles: the influence of size, shape and dielectric environment. J Phys Chem B 107:668–677
3. Gersten J, Nitzan A (1980) Electromagnetic theory of enhanced Raman scattering by molecules adsorbed on rough surfaces. J Chem Phys 73:3023–3037
4. Jackson JB, Westcott SL, Hirsch SL, West JL, Halas NJ (2003) Controlling the surface enhanced Raman effect via the nanoshell geometry. Appl Phys Lett 82:257–259
5. Von Raben KU, Chang RK, Laue RL (1981) Surface study with lasers. Chem Phys Lett 79:465–469
6. Maier S (2007) Plasmonics: fundamentals and applications. Springer, Berlin
7. Kreibig U, Vollmer M (1995) Optical properties of metal clusters. Springer, Berlin
8. Liu X, Kitamura K, Yu Q, Xu J, Osada M, Takahiro N, Li J, Cao G (2013) Tunable and highly reproducible surface-enhanced Raman scattering substrates made from large-scale nanoparticle arrays based on periodically poled $LiNbO_3$ templates. Sci Technol Adv Mater 14:55011
9. Palik ED (1985) Handbook of optical constants. Academic Press, Orlando
10. Pathak NK, Pandey GK, Ji A, Sharma RP (2015) Study of light extinction and surface plasmon resonances of metal nanocluster: a comparison between coated and noncoated nanogeometry. Plasmonics. doi:10.1007/s11468-015-9978-2
11. Gil-Sanchez JA, Ramos-Garcıa JV (2002) Electromagnetic mechanism in surface-enhanced Raman scattering from Gaussian-correlated randomly rough metal substrates. Opt. Exp. 10:17/879
12. Yin YD, Gao L, Qiu CW (2011) Electromagnetic theory of tunable SERS manipulated with spherical anisotropy in coated nanoparticles. J Phys Chem C 115:8893–8899
13. Holand WR, Hall DG (1984) Frequency shift of an electric-dipole resonance near a conducting surface. Phys Rev Lett 52(12):1041–1044
14. Bohren CF, Huffman DR (1998) Absorption and scattering of light by small particles. Wiley, New York
15. Bedeaux D, Vilieger J (2001) Optical properties of surfaces. Imperial College Press, London
16. Sikdar D, Rukhlenko ID, Cheng W, Premaratne M (2013) Optimized gold nanoshell ensembles for biomedical applications. Nanoscale Res Lett 8(1):142–146
17. Jain PK, Huang X, El Sayed IH, El Sayed MA (2007) Review of some interesting surface plasmon resonance-enhanced properties of noble metal nanoparticles and their applications to biosystems. Plasmonics 2(3):107–118
18. Zhu J, Ren Y, Zhao S, Zhao J (2012) The effect of inserted gold nanosphere on the local field enhancement of gold nanoshell. Mater Chem Phys 133(2):1060–1065
19. Pandey GK, Pathak NK, Ji A, Pathak H, Sharma RP (2016) Study of surface enhanced Raman scattering of single molecule adsorbed on the surface of metal nanogeometries: electrostatic approach. Plasmonics 11:1343–1349
20. Lakowicz JR (2006) Plasmonics in biology and plasmon controlled fluorescence. Plasmonic 1(1):5–33

21. Wu D, Jiang S, Liu X (2011) Tunable Fano resonances in three-layered bimetallic Au and Ag nanoshell. J Phys Chem C 115(48): 23797–23801

22. Hu Y, Fleming RC, Drezek RA (2008) Optical properties of gold–silica–gold multilayer nanoshells. Opt Exp 16(24):19579–19591

23. Wu D, Xu X, Liu X (2008) Tunable near-infrared optical properties of three-layered metal nanoshells. J Chem Phys 129(7):074711

24. Xia X, Liu Y, Backman V, Ameer GA (2006) Engineering sub-100 nm multi-layer nanoshells. Nanotechnol. 17(21):5435–5440

25. Hutter T, Elliott SR, Mahajan S (2013) Interaction of metallic nanoparticles with dielectric substrates: effect of optical constants. Nanotechnol 24(3):035201

26. Atwater HA, Polman A (2010) Plasmonics for improved photovoltaic devices. Nat Mater 9:205–213

27. Jain PK, Kyeong LS, El-Sayed IH, El-Sayed MA (2006) Calculated absorption and scattering properties of gold nanoparticles of different size, shape, and composition: applications in biological imaging and biomedicine. J Phys Chem B 110:7238–7248

28. Xu H, Aizpurua J, Kall M, Apell P (2000) Electromagnetic contributions to single-molecule sensitivity in surface-enhanced Raman scattering. Phys Rev E 62:4318–4324

29. Yoshida K, Itoh T, Tamaru H, Biju V, Ishikawa M (2010) Quantitative evaluation of electromagnetic enhancement in surface-enhanced resonance Raman scattering from plasmonic properties and morphologies of individual Ag nano-structures. Phys Rev B 81:115406